Earthquake Engineering, Tenth World Conference © 1992 Balkema, Rotterdam. ISBN 90 5410 060 5

Dynamic discrete modeling and computer simulation of seismic response of concrete stave silos with structural discontinuity

Y. Sasaki & J. Yoshimura
Hokkaido University, Japan

ABSTRACT: Concrete stave silos are segmental silo structures which are cylindrically assembled from precast concrete blocks and held together by exterior post-tensioned steel hoops. For dynamic analysis of concrete stave silos with such structural discontinuity, a new analytical model called "stave silo element" is developed. A procedure for determining spring stiffness in stave silo elements is also proposed. To verify the validity of stave silo elements and the procedure on the equivalent stiffness and its reduction factor, seismic response analyses of a reduced scale model stave silo are carried out and compared with its experimental results. Furthermore, an effective mass coefficient of of stored material during earthquakes significant in seismic design is obtained on the basis of the experimental results.

1 INTRODUCTION

Concrete stave silos have broadly been utilized in the U.S.A. and Canada because the stave silos are more economical and reasonable when compared with other types of silo structures. Even in seismic regions, large-scale concrete stave silos have been constructed recently as industrial and agricultural storage facilities for various materials such as coal, grain and silage.

The cylindrical wall structure of these concrete stave silos are assembled from precast concrete blocks called "stave" and held together by exterior adjustable steel hoops. It is therefore of primary necessity to clarify the dynamic behavior and seismic safety of concrete stave silos with such the discontinuous wall structure. The purpose of this study is to contrive a new discrete type of analytical model and to simulate the earthquake response behavior of concrete stave silos with structural discontinuity. An effective mass coefficient of stored material during earthquakes is also estimated by comparison with the experimental results of a 1/8-scale model stave silo.

2 DYNAMIC MODEL OF CONCRETE STAVE SILOS

The wall structure of concrete stave silos consists of three principal structural components: staves, hoops and stave joints. In creating an analytical model for dynamic response analysis, staves and hoops are assumed to be rigid bodies and hoop springs equivalent to curved beams, respectively, and the resistant mechanism of stave joints is modeled as the stiffness of springs located among rigid bodies. These fundamental analy-

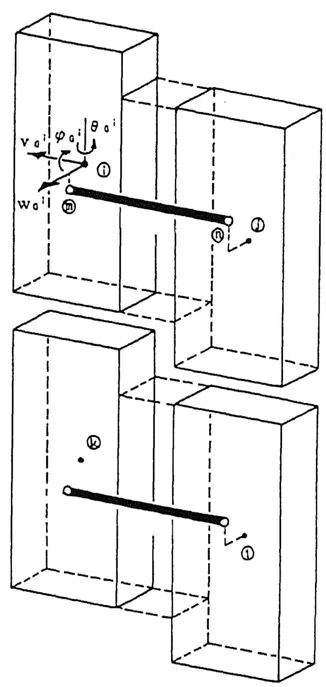

Fig.1 Fundamental analytical models of concrete stave silo structures

tical models of concrete stave silo structures are illustrated in Figure 1.

Fabricating cylindrically the fundamental analytical models and then cutting them by two horizontal planes, a class of finite element named "stave silo element" is defined. As displayed in Figure 2, circular nodal lines are provided on both the sections and a stave silo element has four displacement and rotational angle components along each nodal line.

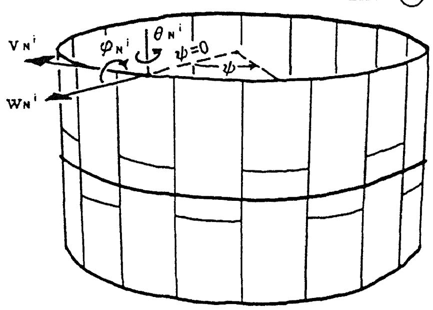

Fig.2 Stave silo element and nodal lines

3 EQUIVALENT SPRING STIFFNESS

It is of primary importance to evaluate the stiffness of springs introduced among rigid bodies in applying stave silo elements. In this study, a procedure for determining the spring stiffness is also proposed. At first, a "continuous" cylindrical shell which has the same material and geometric parameters as a concrete stave silo to be analyzed is considered. The equivalent spring stiffness to the cylindrical shell is then calculated by equations formulated on the basis of shell theory. Furthermore, a reduction factor of the equivalent spring stiffness suitable for the stave silo can be estimated by comparison with experimental results.

Formulas for the equivalent spring stiffness can be expressed as follows:

1. horizontal stave joints;

$$K_v = Eh/2(1+\nu)\ell, \quad K_\theta = Eh^3/3(1+\nu)\ell,$$

$$K_w = Eh^3/2(1+\nu)\ell b^2, \quad K_\phi = 2Eh^3 b/3(1-\nu^2)\ell \qquad (1)$$

2. vertical stave joints;

$$K_v = Eh/(1-\nu^2)b, \quad K_\theta = 2Eh^3 d/3(1-\nu^2)b,$$

$$K_w = Eh^3/2(1+\nu)bd^2, \quad K_\phi = Eh^3 d/3(1+\nu)b \qquad (2)$$

where E and ν are Young's modulus and Poisson's ratio of a cylindrical shell, 2b, 2ℓ and 2h are width, length and thickness of rigid bodies, respectively, and 2d is contact length of adjoining rigid bodies.

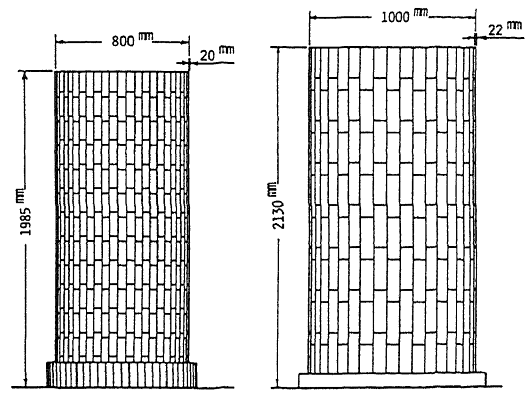

(a) 1/8-scale model: (b) 1/6-scale model:

Fig.3 Two calculation models for verifying the equivalent spring stiffness

Table 1 Comparison of the natural frequencies for lower mode shapes

(a) 1/8-scale model:

	Circumferential wave number, n	Axial wave number, m: 1	2
Cylindrical shell		211	604
Rigid body-spring	1	210	586
(Relative error %)		(-0.5)	(-3.0)
Cylindrical shell		145	398
Rigid body-spring	2	145	398
(Relative error %)		(0.0)	(0.0)

(b) 1/6-scale model:

	Circumferential wave number, n	Axial wave number, m: 1	2
Cylindrical shell		192	536
Rigid body-spring	1	190	497
(Relative error %)		(-1.0)	(-7.3)
Cylindrical shell		127	356
Rigid body-spring	2	128	347
(Relative error %)		(+0.8)	(-2.5)

To verify the accuracy of the formulas (1) and (2), two calculation models illustrated in Figure 3 are considered and free vibration analyses of each calculation model are carried out by both finite element and rigid body-spring methods. Table 1 shows comparisons of the natural frequencies for lower mode shapes of two calculation models. It can be found from Table 1 that the formulas for the equivalent spring stiffness to continuous cylindrical shells provide practically satisfactory accuracy.

4 SIMULATION RESULTS AND COMPARISONS

A series of computer simulation is performed on the seismic response of a 1/8-scale model stave silo, shown in Figure 4, which was designed with satisfaction of similitude requirements (Sasaki and Yoshimura (1989)). This 0.8 m x 2.0 m model stave silo was cylindrically constructed from 650 mortary blocks (15.2 cm x 5.0 cm x 2.0 cm) and 32 steel hoops (4 mm in diameter) on a 2.5 m x 2.5 m shaking table.

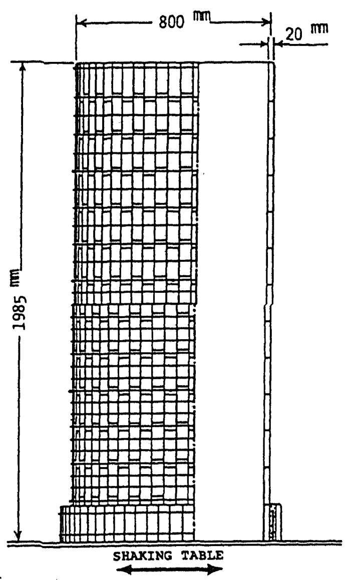

Fig.4 1/8-scale model of a concrete stave silo

One of the input earthquake motions used in the earthquake shaking tests and numerical simulations was derived from the accelerogram of the 1973 Nemurohanto-oki earthquake, but it was speeded up by time scale factor of 8. The peak input accelerations were gradually increased from 0.11 g up to 1.06 g. A time history of the input earthquake acceleraion at an intensity of excitation is displayed in Figure 5.

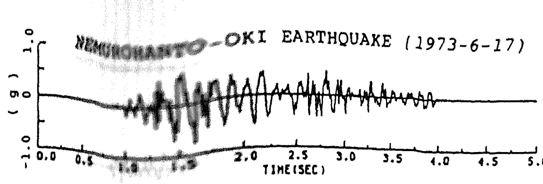

Fig.5 Time history of an input earthquake motion (shaking table acceleration)

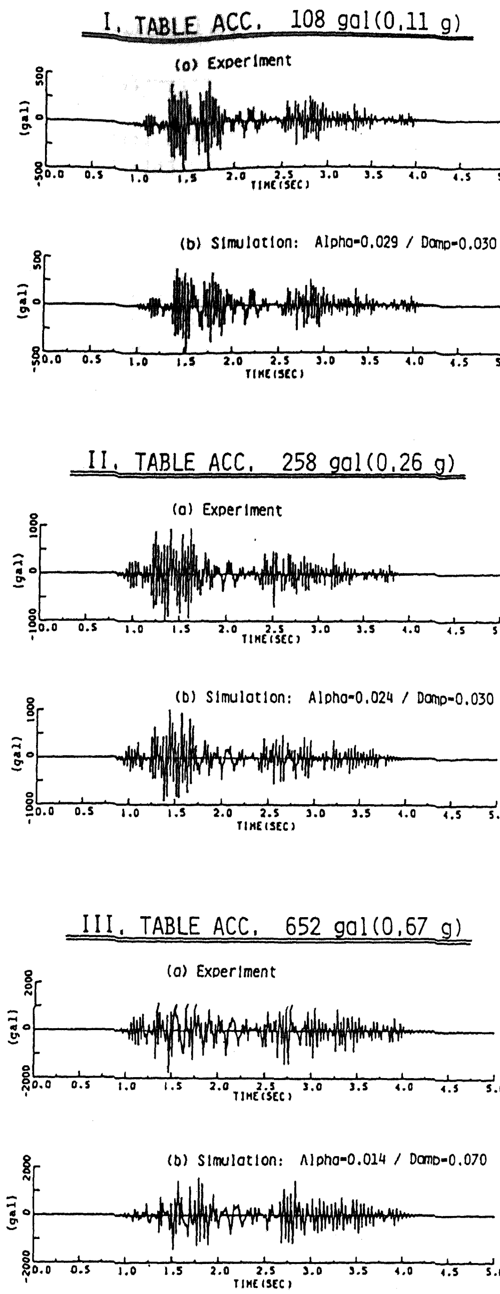

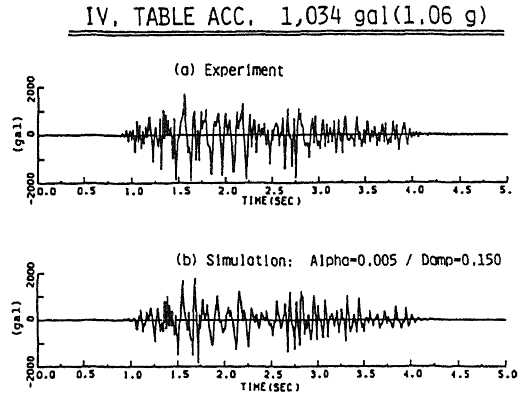

Fig.6 Comparison of earthquake response accelerations at the silo top between the experiment and simulation

Figure 6 shows comparisons of the earthquake response acceleraions at the top of the empty model stave silo for four intensities of excitation; 0.11, 0.26, 0.67 and 1.06 g. Good agreement between the experimental and simulated results demonstrates the validity of stave silo elements and the procedure for the evaluating spring stiffness and its reduction factor. It is also found that nonlinear seismic response characteristics due to the structural discontinuity can sufficiently be simulated even by linearized earthquake response analysis with more appropriate reduction factor at each intensity of excitation.

5 EFFECTIVE MASS COEFFICIENTS

For seismic response analysis, in general, the dynamic effect of stored material is simplified as virtual mass which contributes to inertia force of silo structures. Therefore, the equivalent mass density ρ_e of silo structures including added mass of stored material can be written as

$$\rho_e = \rho_w + C_{eff} \cdot \rho_0 \cdot r \qquad (3)$$

in which ρ_w and ρ_0 are the mass densities of silo structures and stored material, respectively, and r is the ratio of the capacity of stored material to the volume of silo structures per unit height. An effective mass coefficient C_{eff} denotes the ratio of added mass to actual mass of stored material and significant for use in seismic design of silo structures.

5.1 An effective mass coefficient based on the change of natural frequencies

An experimental study on the effective live load of stored material began with the work of Chandrasekaran and Jain (1968) and then shaking tests to confirm their results were carried out by Harris and Nad (1985). In their experimental studies, the coefficients of effective live load or effective weight were decided on the basis of the change of

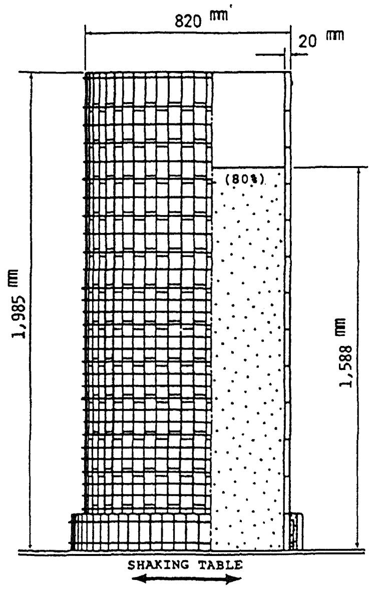

Fig.7 1/8-scale model stave silo filled with a stored material

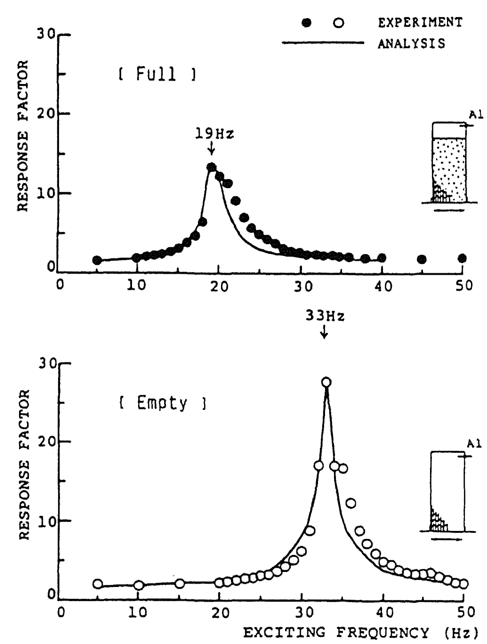

Fig.8 Effect of a stored material on the resonant frequency of the model stave silo

natural frequencies of model silos due to the presence of stored material.

An effective mass coefficient of stored material should be decided by a similar procedure for reference in this study, too. The 1/8-scale model stave silo filled with a stored material (rice) is illustrated in Figure 7. A comparison of the acceleration resonance curves at the top for the model stave silo filled with a stored material or empty is shown in Figure 8. By these experimental results on the fundamental resonant frequencies and free vibration analysis using stave silo elements and the equivalent mass density, the effective mass coefficient under sinusoidal excitation can be decided to be 0.70 (70%).

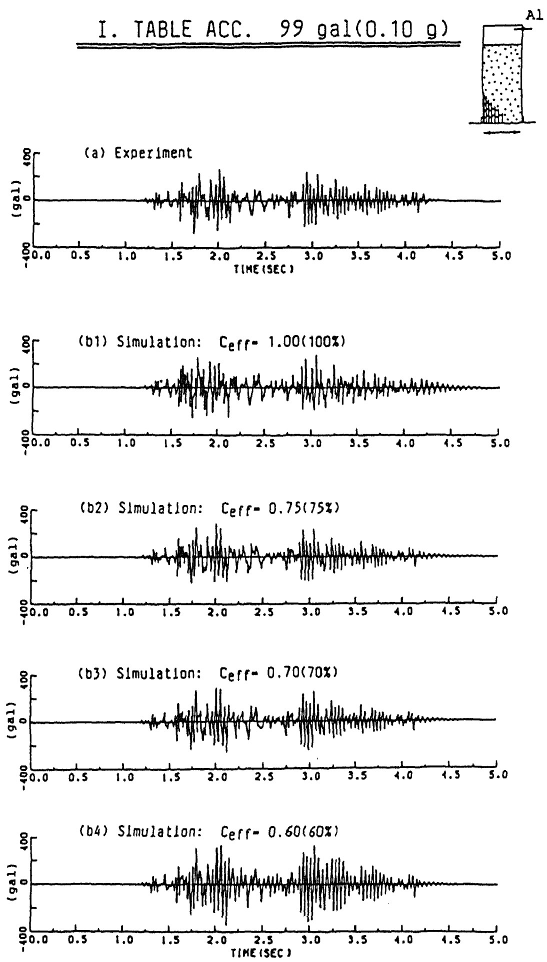

Fig.9 Comparison of earthquake response accelerations at the silo top simulated with several effective mass coefficients

5.2 An effective mass coefficient during earthquakes

Although effective mass coefficients are considerably important in seismic design of silo structures, there are few studies based on earthquake shaking tests and seismic response analyses. For this reason, computer simulation is also performed on the seismic response of the 1/8-scale model stave silo filled with a stored matrial displayed in Figure 7.

Figure 9 shows a comparison of the earthquake response accelerations at the silo top between the experimental and simulated results for the intensity of excitation, 0.10 g. The simulated results from (b1) to (b4) in the Figure 9 are calculated with the different values of effective mass coefficients. Figure 10 presents a similar comparison of the Fourier amplitude spectra of the earthquake response accelerations shown in Figure 9. It must be rather difficult to estimate the most appropriate value of effective mass coefficients even at 5% intervals from Figures 9 and 10.

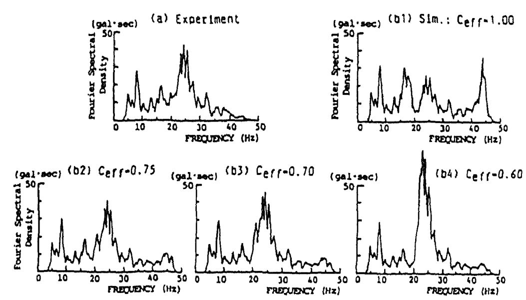

Fig.10 Fourier amplitude spectra of the earthquake response accelerations

In order to evaluate the degree of agreement between the experiment and simulation quantitatively, the following weighted mean relative errors of the Fourier amplitude and phase angle of earthquake response accelerations are introduced in this study.

$$E_A = \Sigma ABS((X^s{}_k - X_k)/X_k) * (X_k/\Sigma X_k)/n_f \qquad (4)$$

$$E_p = \Sigma ABS((\Phi^s{}_k - \Phi_k)/\Phi_k) * (X_k/\Sigma X_k)/n_f \qquad (5)$$

where X_k, Φ_k and $X^s{}_k$, $\Phi^s{}_k$ are the components of the Fourier amplitudes and phase angles of response accelerations obtained by the experiment and simulation, respectively, and n_f is the number of the components. Figure 11 shows the variations of normalized relative errors e_A, e_p with effective mass coefficients. It can easily be found from Figure 11 that the most appropriate value of effec-

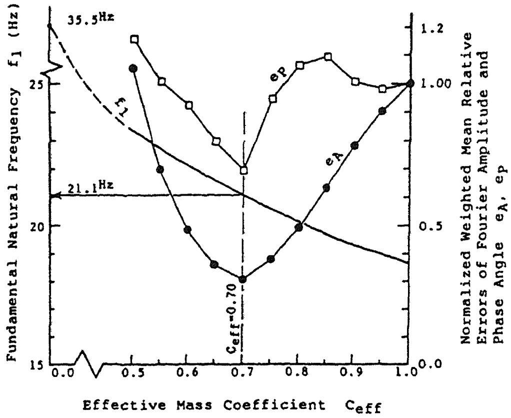

Fig.11 Variations of the evaluation indices with effective mass coefficients

tive mass coefficients during earthquakes is 0.70 (70%) at 5% intervals.

6 CONCLUSIONS

By using stave silo elements and a procedure for determining the equivalent stiffness and its reduction factor proposed in this study, the seismic response of concrete stave silos with structural discontinuity can be simulated with sufficient accuracy. An effective mass coefficient of stored material during earthquakes available for seismic design is also obtained on the basis of experimental results and a couple of evaluation indices.

REFERENCES

ACI Committee 313 1983. Recommended practice for design and construction of concrete bins, silos, and bunkers for storing granular materials (ACI 313-77) and commentary (Revised 1983). American Concrete Institute.

Chandrasekaran, A.R. and P.C. Jain 1968. Effective live load of storage materials under dynamic conditions. Indian Concrete Journal 42: 364-365.

Harris, E.C. and J.D. von Nad 1985. Experimental determination of effective weight of stored material for use in seismic design of silos. ACI Journal 82: 828-833.

NSA Committee 1974. Design standards for concrete stave farm silos. National Silo Association.

Sasaki, Y. and J. Yoshimura 1984. Dynamic behavior of concrete stave silos. Proc. of the Eighth World Conference on Earthquake Engineering, Vol.6, San Francisco: 937-944.

Sasaki, Y. and J. Yoshimura 1989. Seismic response of concrete stave silos with structural discontinuity. Proc. of the Ninth World Conference on Earthquake Engineering, Vol.6, Tokyo & Kyoto: 849-854.

The Farm and Horticultural Building Industry Standards Committee 1974. Specification for cylindrical forage tower silos and recommendations for their use (BS 5061). British Standards Institution.